JOURNAL INDIAN ASSOCIATION OF SEDIMENTOLOGISTS ISSN NO 2582 – 2020
Vol. 41, Issue I, 2024, pp. 22 – 30
DOI: https://doi.org/10.51710/jias.v41iI.331

Constraining provenance and age of the siliciclastic rocks from the south-western Bundelkhand Craton, Central India

M.E.A. Mondal*, Kamaal Parvez, Iftikhar Ahmad and Wamiq Mohammed Khan
Department of Geology, Aligarh Muslim University, Aligarh 202002 (India)
*E-mail Address: meamondal.gl@amu.ac.in

ABSTRACT

The lithology of the Bundelkhand craton, central India, includes highly deformed tonalite, trondhjemite and granodiorite (TTG) gneisses (3.55–2.7 Ga), followed by volcano-sedimentary greenstone belts and a suite of undeformed granitoids ranging in age from 2.52 to 2.49 Ga. The granitoids, which are by far the most dominant lithology of the craton, have intruded into the TTG gneiss-greenstone assemblage. In addition to huge granitic bodies, rhyolitic rocks of 2.54 Ga have also been observed in the Bundelkhand craton. In this study, we report the first occurrence of a small isolated outcrop of siliciclastic sedimentary rocks within the Bundelkhand granitoid suites in and around the Panchwara village, in the southwestern part of the craton. These siliciclastic sedimentary rocks are intruded by the youngest granitic phase of the Bundelkhand granitoid suite, dated as 2.49 Ga old. Thus, their age is determined to be older than 2.49 Ga. Petrographic studies suggest that these rocks are arkose in nature and geochemical composition indicates that they were derived from the older gneiss-greenstone successions and the older granitic phase (2.52 Ga) of the Bundelkhand granitoid suite. The REE modelling suggests that the sediment contribution from different sources is: 50% greenstone belt (15% basalt + 35% sedimentary rocks), 35% gneisses and 15% older granitoids. Detrital zircons from these sedimentary rocks reveal two age populations: one group of zircons is clustering around 2.52 Ga and the other group is ranging from 3.0 to 3.3 Ga indicating at least two protoliths for these sediments. Our field, petrographical and geochemical data, coupled with previously studied zircon geochronological data, is best explained by a model involving deposition of sediments derived from TTG gneiss, greenstone belt and also from the older phase of the granitoid suite. It is interesting to note that the basin received sediments from the older granitic phase of 2.52 Ga age and was closed before the emplacement of the youngest granitic phase at 2.49 Ga. This study, thus, provides for the first time, conclusive evidence for the presence of a late Archean sedimentary basin within the Bundelkhand craton. It is proposed that the sediments were deposited penecontemporaneously with the pulses of the granitoid magmatism in the Bundelkhand Craton that took place ~2.5 Ga.

Keywords: Geochemistry, provenance, modal components, clastic rocks, mineralogy

INTRODUCTION

In most of the cratons, the Archean sedimentary rocks mainly occur as a constituent component of Archean greenstone sequences. However, a few Archean cratons preserve sedimentary rocks which are not a part of the greenstone sequence. The relatively small number of these sedimentary basins, mainly of late Archean age, may point to their low preservation potential. These late Archean sedimentary sequences are distinct in that they are relatively less deformed than their counterparts in the greenstones. The relatively less deformed nature of these sedimentary sequences may give a deceptive notion of the Proterozoic age. These sedimentary basins constitute an essential aspect of Precambrian crustal evolution with respect to provenance characterization and geodynamic setting during late Archean time. In this study, we report field occurrence, petrographical, geochemical data along with previously reported zircon geochronological data of a relatively small outcrop of siliciclastic sedimentary rocks from the south-western part of the Bundelkhand craton (Fig. 1). The objective of this study is to characterize their provenance, paleoweathering condition and to decipher their tectonic setting.

GEOLOGICAL SETTING

The Central Indian Tectonic Zone (CITZ), trending ENE-WSW, separates the Indian land mass into two parts, the northern and southern blocks. The northern block consists of Aravalli and Bundelkhand Cratons and the southern block consists of Singhbhum, Dharwar and Bastar Cratons (Acharyya, 2003; Radhakrishna and Naqvi, 1986). The Bundelkhand Craton is located in the north-central part of India, covering an area of approximately 26000 km^2. It comprises almost 90% of granitoids that are intruded into the older gneisses-greenstone belt. The oldest lithological unit

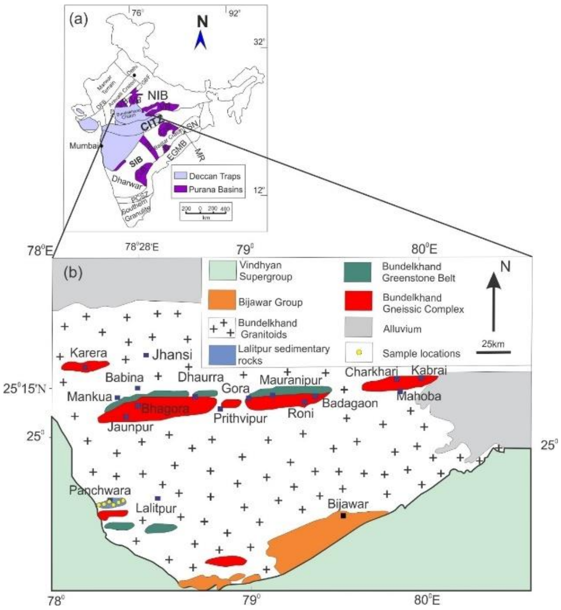

Fig. 1. (a) Map of India showing various major cratons (after Meert and Pandit, 2015). (b) Geological map of Bundelkhand Craton (after Basu, 1986) showing sample locations. ChB: Chhattisgarh Basin; CITZ: Central Indian Tectonic Zone; CuB: Cuddapah Basin; EGMB: Eastern Ghats Mobile Belt; GBF: Great Boundary Fault; IB: Indravati Basin; MB: Marwar Basin; MR: Mahanadi Rift; NIB: North Indian Block; SIB: South Indian Block; PCSZ: Palghat-Cauvery Shear Zone; PG: Pranhita–Godavari Basin; SN: Singhbhum Craton; and VB: Vindhyan Basin

of the Bundelkhand Craton is the tonalite-trondhjemite-granodiorite (TTG) gneisses, which have U-Pb zircon ages of 3.55-2.7 Ga (Mondal et al., 2002; Kaur et al., 2014, 2016). These granite gneisses are overlain by the volcano-sedimentary greenstone complexes. In the Bundelkhand Craton, two greenstone complexes are identified, out of which one is exposed near Girar and Baraitha at the southern edge of the craton known as southern Bundelkhand Greenstone Complex (SBGC) and the other one is exposed at the central part of the craton known as central Bundelkhand Greenstone Complex (CBGC) or Babina-Mauranipur greenstone belt (Malviya et al., 2006). The main litho-units of the SBGC are quartzite, ultramafics and Banded Iron Formation (BIF). The CBGC mainly consists of high-Mg metabasic rocks, ultramafics, BIF, and felsic volcanics. Three types of undeformed granitoids are present in the Bundelkhand Craton: (i) hornblende bearing granitoids (ii) biotite bearing granitoids and (iii) leucogranitoids. The hornblende bearing granitoids and biotite bearing granitoids are similar in age and have emplacement ages of 2516±4 Ma and 2521±7 Ma, respectively obtained by ion microprobe $^{207}Pb/^{206}Pb$ from zircon grains (Mondal et al., 2002). The leucogranitoid phase is slightly younger and has a crystallization age of 2492±10 Ma (Mondal et al., 1998, 2002). These leucogranitoids are intrusive in the isolated small clastic sedimentary basin in and around Lalitpur (Fig. 1b, Fig. 2c). Numerous quartz veins trending NE-SW and NNE-SSW and younger mafic dyke swarm trending NW-SE (~2.0 Ga; Pradhan et al., 2012) and ENE-WSW (~1.1 Ga; Pradhan et al., 2012) have been observed in the Bundelkhand Craton.

SAMPLING AND ANALYTICAL METHODS

Relatively six medium to coarse-grained sedimentary rocks were collected from small isolated outcrop in and around Panchwara village, Lalitpur of Bundelkhand Craton (Fig. 2). During sampling, weathered and jointed surfaces with quartz veins and other lithological contact surfaces were avoided. Thin sections were prepared and the petrographic study was carried out at the Department of Geology, Aligarh Muslim University (AMU), Aligarh using a petrological microscope (Olympus BX-51). The mineralogical composition of the arkose was determined by modal analysis using the Gazzi-Dickinson method (Gazzi 1966; Dickinson 1970). During the modal analysis, we counted more than 400 points and recalculated it on a matrix-free basis. This recalculated data is plotted in the Qt-F-L diagram given by Dickinson et al., (1983). Chips were made ~2-3 cm by using steel mortar and then pulverized up to ~200 mesh (~74 µm) powder by using a tungsten carbide ball mill (FRITSCH pulverisette) in the Department of Geology, AMU. The major oxides have been measured by X-ray fluorescence (XRF; model: Panalytical Axios-mAX) by using pressed pellets at the CSIR-National Geophysical Research Institute (NGRI), Hyderabad with precision of < 2%. Trace elements were determined by High-Resolution Inductively Coupled Plasma Mass Spectrometry (HR-ICP-MS; Model: Nu Instruments Attom, UK), CSIR-NGRI, Hyderabad with precision <10%.

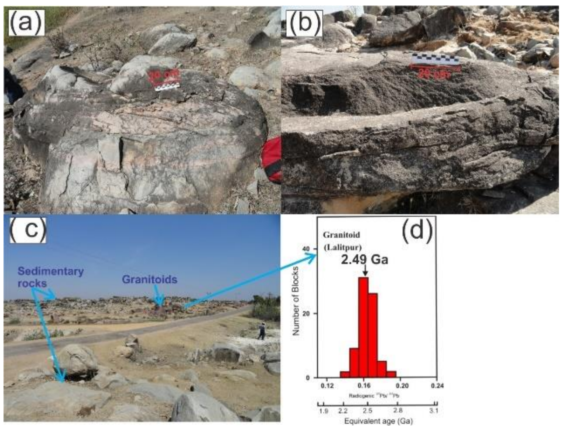

Fig. 2. Field photograph (a) showing a close-up view of the siliciclastic sedimentary rocks (arkose) exposed in the Panchwara village, Lalitpur, (b) showing cross-bedding at Panchwara village, Lalitpur, (c) showing intrusion of 2.49 Ga granitoid into the arkose at the Panchwara village, Lalitpur, (d) histogram of radiogenic $^{207}Pb/^{206}Pb$ block data of zircons from the intruding granitoids (Mondal et al., 1998, 2002).

PETROGRAPHY

The petrographic study suggests that these arkoses range in size from fine to medium-grained and mainly consist of polycrystalline quartz, monocrystalline quartz, plagioclase and microcline (Fig. 3). The polycrystalline quartz is a mosaic of quartz grains and suggests that they are derived from the deformed metamorphosed terrain. The monocrystalline quartz shows undulatory extinction. The quartz grains are angular to sub-rounded in nature and show undulatory extinction. The plagioclase grains are fresh, showing lamellar twinning and no alteration is observed. The microcline is identified by the cross-hatched twinning. The petrographic evidences suggest that they are dominant by first-cycle siliciclastic sediments. The petrography of the arkose rocks is examined in detail to delineate the provenance and tectonic setting. Petrography of the clastic sedimentary rock is important to identify the source and tectonic setting of the sediments (Dickinson et al., 1983). The studied samples are dominated by quartz (average 62%). Polycrystalline quartz is the dominant type (average 65%). Feldspar content in the studied rocks averages 37%. Based on the mineralogy a Q-F-R diagram (Folk, 1980) is constructed, on this plot the rocks are classified as arkose type (Fig. 4).

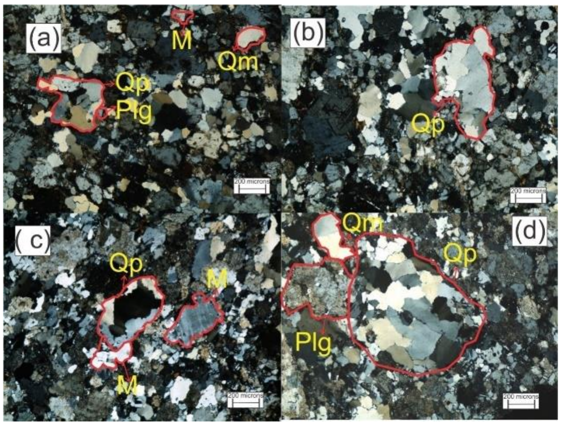

Fig. 3. Photomicrographs showing Lalitpur sedimentary rocks consisting of Qp - polycrystalline quartz; Qm – monocrystalline quartz; Plg – plagioclase; M – microcline

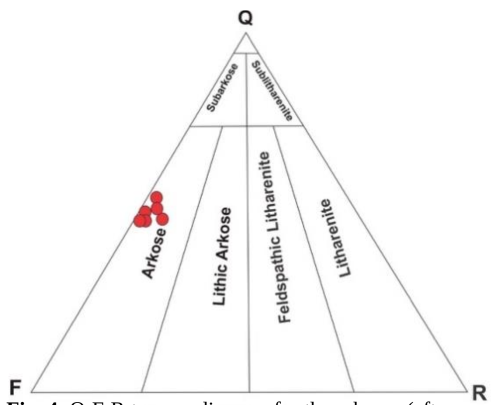

Fig. 4. Q-F-R ternary diagram for the arkoses (after Folk, 1980). Q - total quartz; F - total feldspar; R - total rock fragments including chert.

GEOCHEMICAL DATA

The geochemistry data of the six arkose samples are listed in Table 1. The SiO_2 content varies from 70.5 to 73.9 wt.% with an average of 72.2 wt.% and the Al_2O_3 has high values ranging from 14.0 to 15.6 wt.% (average = 14.8 wt.%). The concentration of $Fe_2O_3^T$ is low ranging from 1.77 to 1.97 wt.% (average = 1.89 wt.%). The concentration of K_2O and Na_2O ranges from 3.01 to 5.99 wt.% (average = 4.05 wt.%) and 3.54 to 4.98 wt.% (average = 4.46 wt.%), respectively. The Na_2O/K_2O ratio values are ranging from 0.59 to 1.63 (average = 1.17). The SiO_2/Al_2O_3 ratio ranges from 4.52 to 5.19 (average = 4.90).

Trace element content is very important to understand the composition of the source rock and the weathering conditions of the clastic rocks, because they are not significantly affected during transportation and post-depositional processes such as diagenesis and metamorphism (Rollinson, 1993; Taylor and McLennan, 1985). The arkoses are characterized by medium to higher concentrations of large ion lithophile elements (LILE; Rb and Ba) with respect to Upper Archean Crust (UAC; Taylor and McLennan, 1985). Relative to UAC, the concentration of Rb varies from 75 to 217 ppm (avg. = 129 ppm; avg. UAC = 50ppm). The Ba concentrations are relatively very high, ranging from 562-694 ppm (average = 640 ppm; avg. UAC = 265ppm). In terms of high field strength elements (HFSE; Zr, Hf), the arkoses are characterized by moderate to high Zr ranging from 93 to 245 ppm (avg. = 148 ppm; avg. UAC = 125ppm) and slightly higher Hf ranging from 3 to 8 ppm (avg. = 4 ppm; avg. UAC = 3ppm). The transition trace elements (TTE) such as Sc, Ni and Cr are lower in the arkoses of this study when compare with UAC. The concentration of Sc, Ni and Cr ranges from 1.6 to 1.9 ppm (avg. = 1.7 ppm; avg. UAC = 14ppm), 3-6 ppm (avg. = 4 ppm; avg. UAC = 105ppm) and 3-5 ppm (avg. = 4 ppm; avg. UAC = 180ppm), respectively, are quite lower (Taylor and McLennan, 1985).

The chondrite normalized (McDonough and Sun, 1995) rare earth element (REE) patterns of

Fig. 5. Chondrite normalized rare earth elements (REE) pattern of the arkoses (after McDonough and Sun, 1995).

Table 1: Major, trace, and rare earth element concentrations for the Lalitpur arkose rocks

Elements	LS101	LS139	LS102	LS104	LS140	LS137
SiO_2 (wt. %)	70.97	70.46	73.87	72.67	73.16	72.26
TiO_2	0.18	0.21	0.28	0.22	0.25	0.19
Al_2O_3	14.89	15.6	14.67	14.01	14.37	14.99
$Fe_2O_3{}^T$	1.86	1.96	1.85	1.97	1.94	1.77
MnO	0.06	0.03	0.05	0.02	0.04	0.03
MgO	0.62	0.45	0.54	0.51	0.24	0.41
CaO	1.85	1.95	0.97	2.13	0.69	2.3
Na_2O	4.98	4.71	3.86	4.78	3.54	4.9
K_2O	4.12	4.12	3.07	4.01	5.99	3.01
P_2O_5	0.02	0.07	0.08	0.04	0.04	0.06
Sum	99.6	99.6	99.2	100.4	100.3	99.9
Sc (ppm)	1.89	1.61	1.87	1.56	1.66	1.59
V	6.10	8.69	7.90	8.01	5.25	7.56
Cr	3.90	4.23	4.98	3.21	3.69	4.35
Co	21.98	27.91	25.98	27.98	21.28	30.19
Ni	3.87	5.81	3.71	5.01	2.85	4.83
Cu	1.05	1.04	0.98	1.03	0.96	1.04
Zn	16.07	22.52	17.93	19.01	16.27	11.08
Ga	14.76	14.21	13.98	15.03	15.19	13.33
Rb	98.04	93.90	211.87	76.76	217.69	75.93
Sr	235.96	236.62	64.92	241.98	64.26	242.82
Y	5.92	5.81	22.89	7.88	23.59	7.81
Zr	102.89	103.35	244.78	96.78	245.32	93.30
Nb	4.76	4.47	17.98	5.43	17.04	5.22
Cs	1.31	1.35	1.71	1.73	1.72	1.71
Ba	692.91	693.76	662.19	615.17	562.27	614.85
La	23.12	21.93	70.21	20.09	70.42	20.54
Ce	37.94	37.59	160.23	36.85	162.59	35.78
Pr	3.61	3.55	13.01	3.78	12.22	3.44
Nd	12.09	12.52	41.01	12.94	40.48	12.10
Sm	1.96	1.95	6.01	1.89	6.21	1.91
Eu	0.68	0.70	0.65	0.64	0.69	0.62
Gd	1.52	1.52	5.01	1.62	5.04	1.58
Tb	0.20	0.19	0.67	0.23	0.68	0.22
Dy	1.05	1.06	4.11	1.40	4.13	1.33
Ho	0.12	0.12	0.43	0.16	0.46	0.15
Er	0.33	0.37	1.65	0.62	1.60	0.52
Tm	0.03	0.05	0.22	0.05	0.21	0.07
Yb	0.46	0.47	2.31	0.89	2.17	0.69
Lu	0.06	0.08	0.43	0.13	0.35	0.12
Hf	3.02	3.02	7.69	2.87	7.49	2.78
Ta	1.26	1.26	2.18	2.06	2.17	2.06
Pb	22.87	21.04	36.62	16.99	35.28	16.00
Th	4.75	4.45	26.89	4.89	27.12	4.84
U	1.05	1.05	4.86	3.87	4.84	1.86
Total REE	83.10	82.00	305.52	81.16	306.89	78.96
$(La/Sm)_N$	7.37	7.02	7.30	6.64	7.08	6.71
$(La/Yb)_N$	34.44	31.83	20.65	15.33	22.08	20.14
$(Gd/Yb)_N$	2.70	2.62	1.75	1.47	1.88	1.85
Eu/Eu*	1.20	1.24	0.36	1.12	0.37	1.09

REE – rare earth elements; $Eu/Eu^* = Eu_N/[(Sm_N) x (Gd_N)]^{1/2}$; $_N$ = chondrite-normalized value (after McDonough and Sun, 1995) the arkoses are characterized by highly fractionated patterns (Fig. 5) with an average $(La/Yb)_N$ ratio of 24.1 (~ 15.3-34.4). The total REE abundance ranges from 79 to 306.9 ppm (avg. = 156.3 ppm). The light rare earth elements (LREE) are moderately enriched in the studied rocks and $(La/Sm)_N$ ratios range from 6.64 to 7.37 with an average value of 7.02. However, heavy rare earth elements (HREE) are relatively less enriched and the $(Gd/Yb)_N$ ratio varies from 1.47 to 2.70 with an average value of 2.05. The Eu anomaly of the is highly variable, ranging from 0.36 to 1.24.

DISCUSSION

PROVENANCE CHARACTERIZATION

The field relationship indicates that the arkoses are intruded by the granitoids, which yielded an age of 2.49 Ga (Mondal et al., 1998, 2002), suggesting that they are older than 2.49 Ga (Fig. 2a). So, these granitoids are not a plausible source for the Lalitpur sedimentary rocks. As documented by Mondal et al. (1998, 2002), based on the geochronology, arkose rocks consist of two age groups of zircon grains viz. one group is clustering around 3.3-3.0 Ga and the other group is clustering around 2.52 Ga. These reported ages are indicating that the possible source of these arkoses is Bundelkhand gneisses (~ 3.55 - 2.7 Ga), volcano-sedimentary greenstone sequence (~2.7-2.5 Ga) and older granitoids phase (~2.52 Ga; Mondal et al., 1998, 2002; Kaur et al., 2014; Singh and Slabunov, 2015).

The concentration of immobile or less mobile elements such as Al, Ti, Zr, Cr, Th, Sc, Co, and La during weathering processes can be used to identify the source rock of the clastic sediments (Cullers, 2002; McLennan and Taylor, 1991). The Al_2O_3 / TiO_2 ratio is used as an indicator of the source rock composition of the clastic sediments. The Al_2O_3/TiO_2ratio in igneous rocks increases with increasing SiO_2 content (Hayashi et al., 1997; Sugitani, 1996). Generally, mafic rocks have Al_2O_3/TiO_2 ratio of <20, whereas that of felsic rocks range from 10 to 100 (occasionally even higher; Hayashi et al., 1997). The Al_2O_3/TiO_2 ratios of the arkose rocks vary from 52.39 to 82.72 (average = 68.24) indicating their felsic affinity. The higher concentration of trace elements such as Th, Zr and La are the indicators of a felsic source, whereas elements such as Co, Cr and Sc are the indicators of a mafic source. The ratios Th/Sc, La/Sc, Th/Co and Cr/Th are used as a powerful tool to delineate the provenance of the clastic sediments (Cullers, 1994; Wronkiewicz and Condie, 1990). The studied rocks have Th/Sc ratio ranging from 2.51 to 16.33 (average = 7.03; for coarse fraction, mafic source = 0.05-0.22, felsic source = 0.84-20.5; Cullers, 2000), La/Sc ratio varies from 12.2 to 42.4 (average = 21.9; for coarse fraction, mafic source = 0.43-0.86, felsic source = 2.5-16.3; Cullers, 2000), Th/Co ratio ranges from 0.16 to 1.27 (average = 0.50; for coarse fraction, mafic source = 0.04-1.4, felsic source = 0.67-19.4; Cullers, 2000) and Th/Cr ratio from 1.05 to 7.35 (average = 2.94; for coarse fraction, mafic source = 0.018-0.046, felsic source = 0.13-2.7; Cullers, 2000). These elemental ratios indicate that sediments are derived from the heterogeneous source, dominantly from the felsic source but there must be some contribution of a mafic source. REE patterns of clastic rocks is a robust tool for deciphering the source rocks (Nesbitt, 1979; Taylor et al., 1986). The REE patterns of arkose have high $(La/Yb)_N$ ratios ranging from 15.33 to 34.4 indicating variable fractionation, supporting the heterogenous source of the clastic sediments. However, these high values suggest that the contribution from the highly fractionated rocks is dominant. The higher values of Eu/Eu^* suggest that the contribution of sediments from the mafic source, whereas lower values of Eu/Eu^* suggest that sediments are derived from the felsic source (Cullers, 2000). The Eu/Eu^* values of the studied rocks range from 0.36 to 1.24, which may indicate the combination of mafic and felsic sources, thus supporting the heterogeneous source of the sediments.

The REE modelling is useful to determine the contribution of the probable sources. We have taken TTG, greenstone belt (basalt + sedimentary rocks) and older granite end members to ascertain their proportions in the arkose rocks. After performing the mixing calculations, it is observed that average sediments are derived from a provenance that consists of 35% TTG, 35% sedimentary rocks of the greenstone belt, 15% basalts of the greenstone belt and 15% of older granitoids (hornblende bearing granitoid and biotite bearing granitoids). These model values are

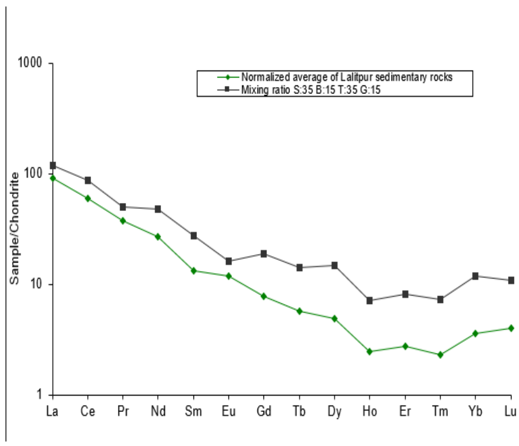

Fig. 6. REE modelling results for estimating the provenance of arkoses after mixing end members in the proportion of 35S:15B:35T:15G (S – sedimentary rocks from the greenstone belt; B – basalts from the greenstone belt; T – TTG gneisses; G – older granitoids.

approximately matched with that of the arkoses (Fig. 6).

PALEOWEATHERING AND PALEOCLIMATE

Several authors attempted to understand paleoweathering and paleoclimate by using different chemical parameters but the most widely used parameter to quantify the paleoweathering intensity is the chemical index of alteration (CIA), which indirectly leads to clues about paleoclimate conditions. Nesbitt and Young (1982) proposed the parameter CIA to evaluate the chemical weathering of the source rock based on the differential solubility of CaO, Na_2O, K_2O and Al_2O_3. CIA can be calculated by taking the molar proportion of the CaO, Na_2O, K_2O and Al_2O_3: CIA = $[Al_2O_3/(Al_2O_3+CaO^*+Na_2O+K_2O)] \times 100$, (molecular proportion), where CaO^* represents the CaO derived from the silicate minerals only. The CIA values of the studied rocks vary from 47 to 56 (average = 50) indicating that they have not undergone significant weathering.

The arkoses are plotted in the A-CN-K diagram (Al_2O_3-CaO^*+Na_2O-K_2O; Nesbitt and Young, 1984) to envisage the paleoweathering trend (Fig. 7). This diagram is helpful to understand the weathering trend because CaO and Na_2O bearing feldspar (plagioclase feldspar) are more easily leached out during chemical weathering than K-feldspar (Middelburg et al., 1988). Thus, the weathered samples give a parallel trend to A-CN axis. The studied samples fall on the tie line which joins the plagioclase feldspar and K-feldspar, indicating moderate weathering effect on the studied rocks. The Th/U ratio is considered a good indicator to assess the paleoweathering condition. U is soluble in water during the weathering and becomes mobile (U^{+4} converts into U^{+6}). Due to the mobility of U, the Th/U ratio is elevated and becomes a good indicator of weathering. If the Th/U is greater than 4, it stipulates that the rocks have gone through the weathering (McLennan and Taylor, 1991; McLennan et al., 1990). The average value of Th/U of the arkose is 3.96, further supporting the insignificant chemical weathering effect on the studied rocks. This may be due to the sedimentation occurring for a very short time period, as discussed earlier. So, mechanical weathering is dominant rather than the chemical weathering.

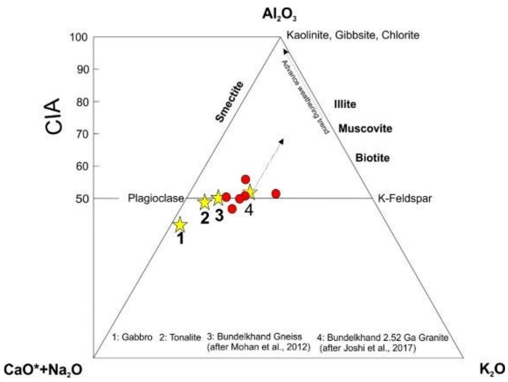

Fig. 7. A-CN-K (in molecular proportion) ternary plot (after Nesbitt and Young, 1984) gives a paleoweathering trend. Average composition is also plotted for comparison from 2.52 Ga Bundelkhand granite (after Joshi et al. 2017) and Bundelkhand gneiss (after Mohan et al. 2012).

TECTONIC SETTING

The tectonic setting of the sedimentary basin can be identified by the geochemistry of the clastic rocks (Verma and Armstrong-Altrin, 2013, 2016). Based on Folk's classification (1980) of sandstone, the studied sedimentary rocks are characterized as arkose (Fig.4). Pettijohn et al. (1987) suggested that arkose is formed at the high relief regions. This condition is generally found at continental rifts. Based on the major oxides chemistry (K_2O/Na_2O vs SiO_2), Roser and Korsch (1986) proposed a tectonic discriminant diagram to depict the tectonic environment from which sediments were derived. The Lalitpur arkoses are plotted in the passive margin field (Fig. 8). Bhatia and Crook (1986) give a tectonic discriminant diagram based on the trace elements Th, Sc and Zr. The trace elements are more trustworthy than the major oxides during post-depositional processes. The arkoses are plotted in the passive margin field in the Th-Sc-Zr/10 ternary diagram, endorsing the rift-related origin of the basin (Fig. 9). The passive margins were characterized by the separation of continents and rifting (Dickinson, 1981). Based on the mineralogy of the sandstone, Dickinson et al. (1983) proposed a Q_t-F-L diagram to discriminate the tectonic setting of the source region. The arkoses plot in the basement uplift field (Fig. 10), indicating that the sediments were derived from the greater relief, further supporting the rifting origin of the basin. Based on the preceding discussion, a plausible model has been proposed for the arkose rocks, which is shown in a schematic cartoon in Fig. 11.

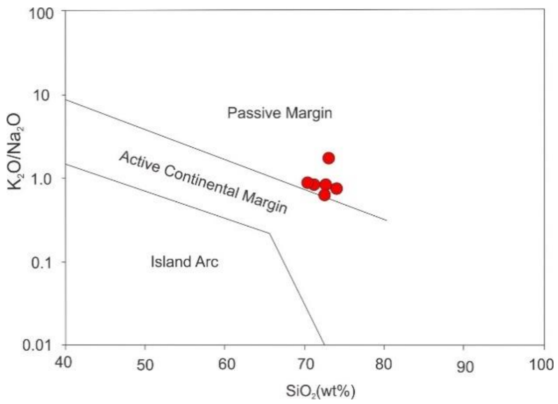

Fig. 8. SiO_2 vs. K_2O/Na_2O binary tectonic discriminant diagram for the arkoses (after Roser and Korsch, 1986).

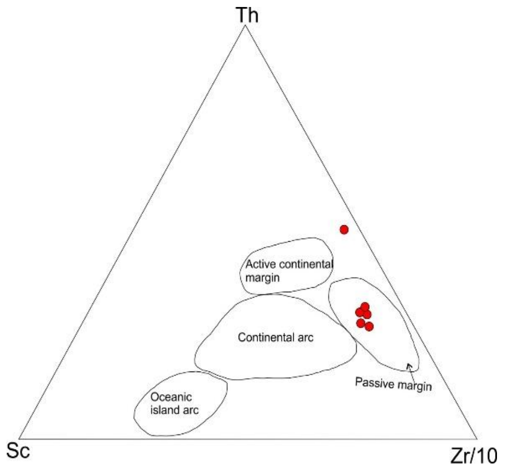

Fig. 9. Th-Sc-Zr/10 tectonic discrimination diagram for the arkoses (after Bhatia and Crook, 1986)

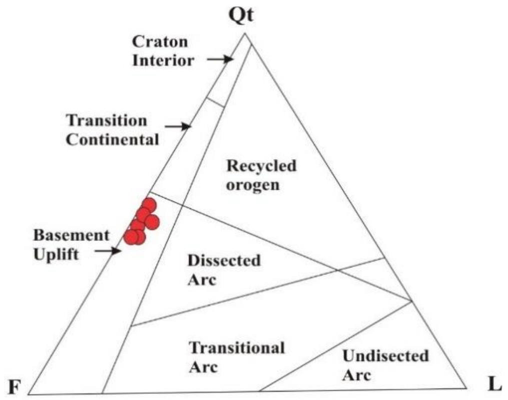

Fig. 10. Qt-F-L ternary diagram for the arkoses, fields are after Dickinson et al. (1983). Qt – total quartz (monocrystalline quartz + polycrystalline quartz); F – total feldspar; L – total lithic fragments

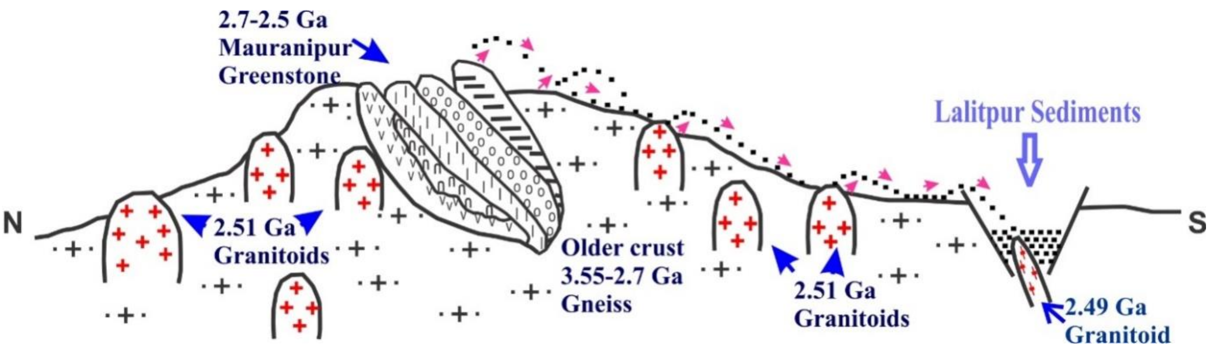

Fig. 11 Schematic diagram showing the contribution of the sediments from different sources (TTG, greenstone belt and granitoids).

CONCLUSION

1. The rocks are classified as arkose type.
2. These arkoses are derived from the TTG gneisses, volcano-sedimentary greenstone sequences and older undeformed granitoids.
3. Based on the REE modelling, the contribution of different sources is depicted as, i.e. 50% greenstone belt (15% basalt + 35% sedimentary rocks), 35% TTG and 15% older undeformed granitoids.
4. The arkoses show insignificant effect of chemical weathering.
5. The compiled data reveal that the Lalitpur basin was developed due to the continental rifting between 2.52 Ga and 2.49 Ga.

ACKNOWLEDGEMENTS

We are thankful to the Chairperson, Department of Geology, AMU, Aligarh and the Director, CSIR-NGRI, Hyderabad for providing facilities to carry out this work.

FUNDING

This work did not receive any external funding.

CONFLICT OF INTEREST

The authors declare no conflict of interest.

REFERENCES

Acharyya, S.K. (2003). The nature of the mesoproterozoic Central Indian Tectonic Zone with exhumed and reworked older granites. Gondwana Research, v. 6, pp. 197-214.

Basu, A.K. (1986). Geology of parts of Bundelkhand granite massif, central India. Records of the Geological Survey, India, v. 11/2, pp. 61-124.

Bhatia, M.R. and Crook, K.A.W. (1986). Trace element characteristics of greywackes and tectonic discrimination of sedimentary basins. Contribution to Mineralogy and Petrology, v. 92, pp. 181-193.

Cullers, R.L. (2000). The geochemistry of shales, siltstones and sandstones of Pennsylvanian-Permian age, Colorado, USA: Implications for provenance and metamorphic studies. Lithos, v. 51, pp. 181-203.

Cullers, R.L. (1994). The controls on the major and trace element variation of shales, siltstones, and sandstones of Pennsylvanian-Permian age from uplifted continental blocks in Colorado to platform sediment in Kansas, USA. Geochimica et Cosmochimica Acta, v. 58, pp. 4955-4972.

Cullers, R.L. (2002). Implications of elemental concentrations for provenance, redox conditions, and metamorphic studies of shales and limestones near Pueblo, CO, USA. Chemical Geology, v. 191, pp. 305-327.

Dickinson, W.R. (1970). Interpreting detrital modes of graywacke and arkose: Journal of Sedimentary Petrology, v. 40, pp. 695-707.

Dickinson, W.R. (1981). Plate tectonic evolution of the southern Cordillera. Arizona Geological Society Digest, v. 14, pp. 113-135.

Dickinson, W.R., Beard, L.S., Brakenridge, G.R., Erjavec, J.L., Ferguson, R.C., Inman, K.F., Knepp, R.A., Lindberg, F.A. and Ryberg, P.T. (1983). Provenance of North Phanerozoic sandstones in relation to tectonic. Geological Society of America Bulletin, v. 94, pp. 222-235.

Folk, R.L. (1980). Petrology of sedimentary rocks. Hemphill publishing company.

Gazzi, P. (1966). Le arenarie del flysch sopracretaceo dell'Appennino modensese: Correlazioni con il flysch di Monghidoro: Mineralogica et Petrographica Acta, v. 12, p. 69-97.

Hayashi, K.I., Fujisawa, H., Holland, H.D. and Ohomoto, H. (1997). Geochemistry of ~1.9 Ga sedimentary rocks from northern Labrador Canada. Geochimica et Cosmochimica Acta, v. 61(19), pp. 4115-4137.

Joshi, K.B., Bhattacharjee, J., Rai, G., Halla, J., Ahmad, T., Kurhila, M., Heilimo, E. and Choudhary, A.K. (2017). The diversification of granitoids and plate tectonic implications at the Archean-Proterozoic boundary in the Bundelkhand Craton, Central India. Geological Society of London Special Publications, v. 449, pp. 123-157.

Kaur, P., Zeh, A. and Chaudhri, N. (2014). Characterization and U-Pb-Hf record of the 3.55 Ga felsic crust from the Bundelkhand Craton, northern India. Precambrian Research, v. 255, pp. 236-244.

Kaur, P., Zeh, A., Chaudhri, N. and Eliyas, N. (2016). Unravelling the record of Archean crustal evolution of the Bundelkhand Craton, northern India using U-Pb zircon-monazite ages, Lu-Hf isotope systematics, and whole-rock geochemistry of granitoids. Precambrian Research, v. 281, pp. 384-413.

Malviya, V.P., Arima, M., Pati, J.K. and Kaneko, Y. (2006). Petrology and geochemistry of metamorphosed basaltic pillow lava and basaltic komatiite in the Mauranipur area: Subduction related volcanism in the Archean Bundelkhand craton, central India. Journal of Mineralogy and Petrology, v. 101, pp. 199-217.

McDonough, W.F. and Sun, S.S. (1995). The composition of the Earth. Chemical Geology, v. 120, pp. 223-253.

McLennan, S.M., Taylor, S.R., McCulloch, M.T. and Maynard, J.B. (1990). Geochemical and Nd-Sr isotopic composition of deep sea turbidites: Crustal evolution and plate tectonic associations. Geochimica et Cosmochimica Acta, v. 54, pp. 2015-2050.

McLennan, S.M. and Taylor, S.R. (1991). Sedimentary rocks and crustal evolution: tectonic setting and secular trends. Journal of Geology, v. 99, pp. 1-21.

Meert, J.G. and Pandit, M.K. (2015). The Archean and Proterozoic history of Peninsular India: Tectonic framework for Precambrian sedimentary basins in India. Geological Society of London, Memoirs, v. 43, pp. 29-54.

Middelburg, J., Vanderweijden, C. and Woittiez, J. (1988). Chemical processes affecting the mobility of major, minor and trace elements during weathering of granitic rocks. Chemical Geology, v. 68, pp. 253-273.

Mohan, M.R., Singh, S.P., Santosh, M., Siddiqui, M.A. and Balaram, V. (2012). TTG suite from the Bundelkhand Craton, Central India: geochemistry, petrogenesis and implications for Archean crustal evolution. Journal of Asian Earth Sciences, v. 58, pp. 38-50.

Mondal, M.E.A., Sharma, K.K., Rahman, A. and Goswami, J.N. (1998). Ion microprobe $^{207}Pb/^{206}Pb$ zircon ages for the gneiss-granitoid rocks from Bundelkhand massif: evidence for the Archean components. Current Science, v. 74, pp. 70-75.

Mondal, M.E.A., Goswami, J.N., Deomurari, M.P. and Sharma, K.K. (2002). Ion microprobe $^{207}Pb/^{206}Pb$ ages of zircons from the Bundelkhand massif, northern India: implications for crustal evolution of the Bundelkhand-Aravalli protocontinent. Precambrian Research, v. 117, pp. 85-100.

Nesbitt, H.W. (1979). Mobility and fractionation of rare earth elements during weathering of a granodiorite. Nature, v. 279, pp. 206-210.

Nesbitt, H.W. and Young, G.M. (1982). Early Proterozoic climates and plate motions inferred from major element chemistry of lutites. Nature, v. 299, pp. 715-717.

Nesbitt, H.W. and Young, G.M. (1984). Prediction of some weathering trends of plutonic and volcanic rocks based on thermodynamic and kinetic considerations. Geochimica et Cosmochimica Acta, v. 48, pp. 1523-1534.

Pettijohn, F.J., Potter, P.E. and Siever, R. (1987). Sand and Sandstone, 2nd ed. Springer, New York, pp. 553.

Pradhan, V.R., Meert, J.G., Pandit, M., Kamenov, G. and Mondal, M.E.A. (2012). Paleomagnetic and geochronological studies of the mafic dyke swarms of Bundelkhand craton, central India:

implications for the tectonic evolution and paleogeographic reconstructions. Precambrian Research, v. 198-199, pp. 51-76.

Radhakrishna, B.P. and Naqvi, S.M. (1986). Precambrian continental crust of India and its evolution. Journal of Geology, v. 94, pp. 145-166.

Rollinson, H.R. (1993). Using geochemical data: Evaluation, Presentation, Interpretation. Longman Singapore Publishers (Pte) Ltd. Singapore, pp 352.

Roser, B.P. and Korsch, R.J. (1986). Determination of tectonic setting of sandstone-mudstone suites using SiO_2 content and K_2O/Na_2O ratio. The Journal of Geology, v. 94(5), pp. 635-650.

Singh, V.K., and Slabunov, A. (2015). The Central Bundelkhand Archean greenstone complex, Bundelkhand craton, central India: geology, composition, and geochronology of supracrustal rocks. International Geology Review, v. 57, pp. 1349-1364.

Sugitani, K. (1996). Anomalously low Al_2O_3/TiO_2 values for Archean cherts from the Pilbara Block, Western Australia-possible evidence for extensive chemical weathering on the early earth. Precambrian Research, v. 80, pp. 49-76.

Taylor, S.R. and McLennan, S.M. (1985). The continental crust. Its Composition and Evolution. Blackwell, Oxford, UK. ISBN 0632011483.

Taylor, S.R., Rudnick, R.L., McLennan, S.M. and Eriksson, K.A. (1986). Rare earth element patterns in Archean high-grade meta sediments and their tectonic significance. Geochimica et Cosmochimica Acta, v. 50, pp. 2267-2279.

Verma, S.P. and Armstrong-Altrin, J.S. (2016). Geochemical discrimination of siliciclastic sediments from active and passive margin settings. Sedimentary Geology, v. 332, pp. 1-12.

Verma, S.P. and Armstrong-Altrin, J.S. (2013). New multi-dimensional diagrams for tectonic discrimination of siliciclastic sediments and their application to Precambrian basins. Chemical Geology, v. 355, pp. 117-133.

Wronkiewicz, D.J. and Condie, K.C. (1990). Geochemistry and mineralogy of sediments from the Ventersdorp and Transvaal Supergroups, South Africa: Cratonic evolution during the early Proterozoic. Geochimica et Cosmochimica Acta, 5v. 4, pp. 343-354.